Crowded Piperidines with Intramolecularly Hydrogen-Bonded Nitrogen: Synthesis and Conformation Study

Anatoly M. Belostotskii,* Hugo E. Gottlieb, and Pinchas Aped[a]

Abstract: 2,2,6,6-Tetramethyl substituted piperidines with a β-branched *N*-alkyl substituent were synthesized by the photoreaction of *N*-Me precursors with ketones. The main conformation features of these sterically-hindered amines (established by NMR and IR spectroscopy) are a ring in the chair form, an eclipsed conformation for the *N*-substituent and an intramolecular OH···N bond. High barriers for the geminal substituent topomerization were measured for these piperidines at different temperatures by means of line-shape analysis of the temperature-dependent ^{13}C and ^{1}H NMR spectra. An MM3-derived conformation scheme indicated that, for one of the studied analogues, the rotation of the *N*-substituent determines a slow topomerization rate. A new mechanism of nitrogen inversion—a concerted hydrogen-bond dissociation/nitrogen inversion process—is considered for hydrogen-bonded amines.

Keywords: amines · conformation analysis · NMR spectroscopy · photooxidation

Introduction

The conformation analysis of monocyclic alkylpiperidines demonstrates that there is no qualitative discrepancy between the thermodynamic conformation features of unhindered and most of the hindered analogues. With few exceptions,[1a–e] the chair form is the preferred piperidine ring conformation and a tendency of the ring substituents to adopt an equatorial orientation determines the conformation equilibrium for mono-, di-, tri-, and polysubstituted piperidines.[2a–f]

In contrast, the conformation dynamics of these cycles are sensitive to the ring substitution. For instance, the low-energy pathways of topomerization of the ring substituents are not equivalent for *N*-Me piperidine **1a** and *N*-Et piperidine **1b** (see Figure 1 and Scheme 1).[3, 4] In consequence, the NMR-measured barriers[3–5] for this topomerization (observed as a doubling of resonance signals of the geminal ring substituents) are appreciably different. In general, it is difficult to predict how the ring crowding would influence the topomerization kinetics. The barriers decrease with an increase of the bulk, such as the *N*-alkyl substituent in some *C*-unsubstituted piperidines **2a**–**c**. In contrast, these barriers increase in other *C*-unsubstituted piperidines[6a,b] as well as in hindered analogues **1b**–**e**. Such barriers are extremely high in spiro compounds **3a** and **3b**.[6c]

[a] Dr. A. M. Belostotskii, Dr. H. E. Gottlieb, Dr. P. Aped
Chemistry Department, Bar-Ilan University
Ramat-Gan 52900 (Israel)
Fax: (+972) 3-535-1250
E-mail: belostot@mail.biu.ac.il

Even for close analogues **1b**–**e** it is difficult to conclude whether a significant increase (more than 3 kcal mol^{-1}) of the topomerization barrier for compound **1e** is due to the increase in the bulkiness of the *N*-substituent, or to the involvement of different intramolecular motions. For instance the latter gives rise to the 4 kcal mol^{-1} difference for piperidines **1a** and **2a**.[3–5]

In this work we discuss the relationship between conformation kinetics and the structure of the *N*-alkyl substituent in piperidines with a sterically hindered amino fragment and also describe their conformation dynamics in terms of conformation schemes. We synthesized 2,2,6,6-tetramethylpiperidines, bearing a β-branched *N*-substituent, measured topomerization rates for analogues with a nonfunctionalized piperidine ring by dynamic NMR (DNMR) spectroscopy, and performed MM3-based calculations in order to identify the rate-determining intramolecular dynamic processes.

Results and Discussion

Synthesis of sterically hindered piperidines

The highly crowded amines **4**–**7** were prepared by using two different approaches (see Scheme 2). The less-hindered **4** was synthesized by the alkylation of secondary amine **8** by isobutyl iodide **9** in 70–80% yield. Attempts to introduce a neopentyl substituent by the alkylation of **8** were unsuccessful. Amine **8** remained unchanged when heated with a 30-fold excess of neopentyl iodide (160 °C, 15 days) or with neopentyl triflate (nitromethane, reflux, 8 h).

  0947-6539/02/0813-3016 $ 17.50+.50/0

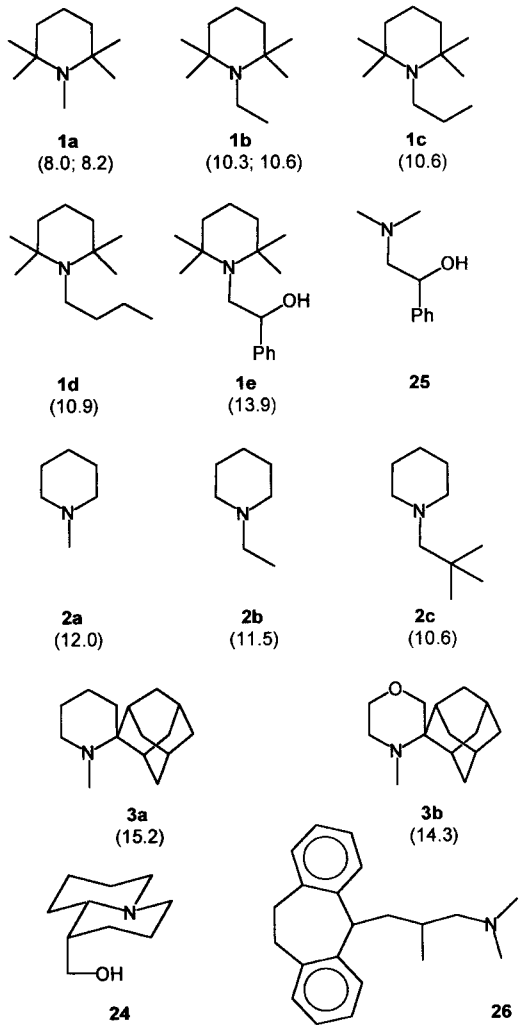

Figure 1. Amines **1a–e**, **2a–c**, **24**, **25** and **26** (the corresponding NMR-measured barriers, kcal mol^{-1}, are in parentheses).

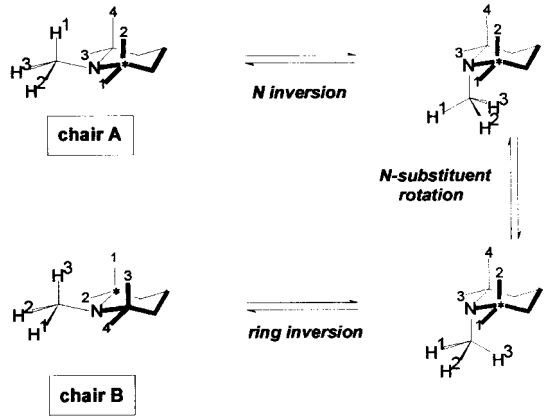

Scheme 1. Three formal intramolecular motions (taken in an arbitrary sequence) which provide the DNMR-observed topomerization chair **A** ↔ chair **B** in piperidines, for example, in piperidine **1a**[4,5] (the asterisk is a formal label, numbers indicate the methyl groups).

Hindered amines **5** and **6**, which possess an intramolecular hydrogen bond (see below), were obtained by a modification of the *N*-methyl substituent of tertiary amine **1a** by photochemical reduction of ketones.[7a] Photolysis of amine **1a** with

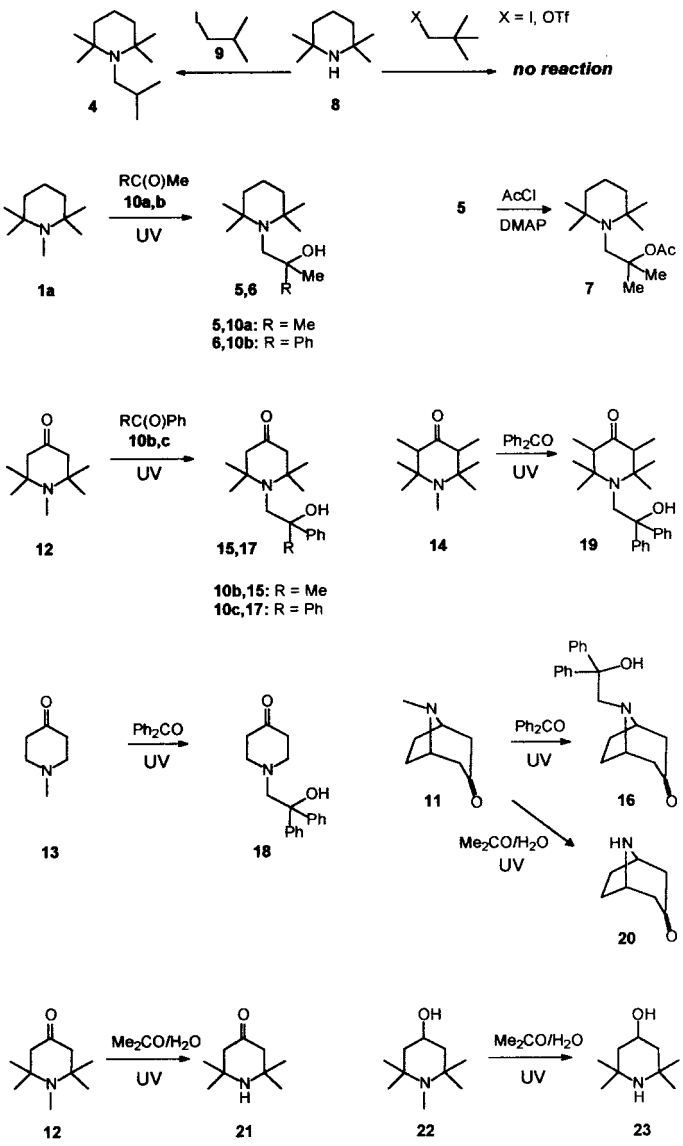

Scheme 2. Piperidine derivatives **1–8**, **11–23**. For photoreactions in benzene (i.e., not in the acetone-water mixture) only the isolated cross-recombination products **5**, **6**, **15–19** are shown.

an excess of acetone **10a** or with acetophenone **10b** in benzene led to **5** and **6** (cross-recombination products[7a,b]) in 20–25% yield. Acetylation of aminoalcohol **5** to acetoxy compound **7** was performed by means of the DMAP-based procedure (DMAP = dimethylaminopyridine).[8a,b] The corresponding trifluoroacetate was formed quantitatively (as observed by NMR spectroscopy) when **5** was acylated by trifluoroacetic acid anhydride (without DMAP). However, this compound was not isolated because of its rapid decomposition on silica into a mixture of the olefinic products of elimination of the trifluoroacetate group (observed by NMR spectroscopy).

We also studied this photoreaction for *N*-Me 4-piperidones (see Scheme 2). These aminoketones possess two photoreactive centers—the amino function and the carbonyl group, which are capable of photooxidation by ketones and photoreduction by amines,[7a] respectively—and, therefore, have more transformation possibilities. In addition, the keto group in aliphatic ketones is, in itself, photolabile.[9] For instance, the

piperidine ring of tropinone (**11**) hydrochloride is opened under UV irradiation[10] due to the photolytic cleavage of the keto fragment (in this case the photoreductive ability of the *N*-Me group is suppressed by the salt formation).

As we now show, the piperidone *N*-methylamino and keto functions interact when the tertiary amino group is not protonated; piperidone **12** is converted in a multicomponent mixture after 8 h irradiation in benzene. In the presence of ketone **10b**, however, **12** gave piperidone **15** in 15% yield. Also, reaction of **11**–**14** with benzophenone (**10c**) led to the corresponding piperidones **16**–**19** in 10–23% yields. A significant part (about 30–40%) of the starting amines **11**–**14** is transformed into the corresponding N-demethylation products, which were only detected by NMR spectroscopy and not isolated.

We found that this photoreaction (for the photodemethylation of amines by ketones see ref. [7a]) may serve as a preparative route to N-demethylation of *functionalized* tertiary methylamines; demethylation yields are increased when an acetone/water mixture is employed as the reducing solvent. If, for example, aminoketones **11** and **12** are irradiated in this mixture, *N*-H compounds **20** and **21** are isolated in 79 and 82% yield, respectively (no appreciable amounts of the dimerization and cross-recombination products[7a,b] were formed). Another example is aminoalcohol **22**. This compound, with two potential photoreducing centers (the tertiary amino[7a] and the secondary hydroxy[11] groups), is chemoselectively converted under the same conditions into secondary piperidole **23** in 72% yield.

Table 1. Data from the ^{1}H NMR[a] (δ_H, J [Hz]) and high-resolution mass spectra (m/z) for piperidines **4**–**7** and **15**.

	α-Me	ring CH_2's	N-CH_2	Others	MH^+ (calcd)
4	0.99 br s	1.3–1.6	2.22	0.85 d, 6.7 (Me)	198.217
			d, 7.2	1.65 th, 7.2, 6.7 (CH)	(198.222)
5	1.05 s	1.4–1.6	2.52 s	1.22 s (2 Me)	214.224
	1.08 s			5.3 br s (OH)	(214.217)
6	0.35 s_e	1.3–1.7	3.00 s	1.47 s (Me) 5.7 br s (OH)	276.215
	0.91 s_a			7.14 m (*p*-H) 7.27 m (*m*-H)	(276.233)
	1.09 s_a			7.41 m (*o*-H)	
	1.19 s_e				
7	0.97 s	1.3–1.7	2.91 s	1.49 s (2 Me)	256.229
	0.98 s			1.94 s (COMe)	(256.228)
15	0.52 s_e	2.14 dd, 12.6, 2.4 (3-H_a)	3.12 s	1.52 s (Me) 5.3 br s (OH)	–
	0.94 s_a	2.48 dd, 12.6, 2.4 (5-H_a)		7.17 m (*p*-H)	
	1.13 s_a	2.54 d, 12.6 (3-H_e)		7.29 m (*m*-H)	
	1.37 s_e	2.66 d, 12.6 (5-H_e)		7.44 m (*o*-H)	

[a] In $CDCl_3$ at 25 °C; h = septet, a = axial, e = equatorial.

Table 2. ^{13}C NMR data for piperidines **4**–**7** and **15** in $CDCl_3$ at 25 °C.

	C-2, C-6	C-3, C-5	C-4	α-Me[a]	C-1′	C-2′	Me	Others
4	54.58	41.67	18.10	28.30 br	52.33	30.90	21.15	–
5	55.16	41.09	17.70	22.32$_a$	54.00	63.57	31.61	–
				35.18$_e$				
6	54.85	40.93	17.62	22.59$_a$	56.85	67.33	33.55	124.60 (*p*)
	55.42	41.02		22.09$_a$				125.37 (*o*)
				34.55$_e$				127.57 (*m*)
				34.65$_e$				152.80 (*i*)
7	54.87	41.59	17.87	21.58$_a$	54.52	85.47	25.79	22.69 (*Me*CO)
				34.90$_e$				170.66 (C=O)
15	59.78	55.47	208.02	24.30$_a$	56.51	67.85	33.50	124.53 (*p*)
	60.30	55.51		23.82$_a$				125.85 (*o*)
				34.48$_e$				128.30 (*m*)
				34.64$_e$				151.99 (*i*)

[a] a = axial, e = equatorial, br = broadened.

NMR and IR spectroscopic study

Conformation analysis: Data for the room-temperature ^{1}H and ^{13}C NMR spectra of compounds **4**–**7** and **15** are given in Tables 1 and 2. Our experimental data support a predominance of the chair conformation for polysubstituted piperidines with a bulky *N*-substituent. In the ^{1}H NMR spectrum of piperidone **15** we can detect a long-range coupling interaction between the axial protons H-3 and H-5 (2.4 Hz), which, being diastereotopic, are chemically nonequivalent. Cyclic ketones only possess such a long-range spin–spin interaction in the chair conformation.[2d] In addition, the chemical shift difference for the geminal protons in the 3- and 5-positions of **17** (0.48 ppm) is the same as the difference for the equatorial and axial protons at C-2 of the conformationally restricted "chair compound" **16** (0.46 ppm).

A preference for the conformation in which the nitrogen atom is intramolecularly hydrogen-bonded was found in aminoalcohols **5**, **6**, and **15**–**19**, as indicated by a very broad signal for the OH proton at room temperature at about 5.5 ppm. The temperature dependence of the OH chemical shift strongly supports this conclusion; heating (for **5** and **6**) causes only a small upfield shift for these signals (< 0.2 ppm/100 °C). This information provides evidence for the presence of an intramolecular hydrogen bond in close analogue **1e**, as claimed in reference [12].

Furthermore, the IR spectra of dilute solutions of compounds **15**–**19** in CCl_4 show broad absorbances centered at 3260, 3372, 3360, 3392, and 3400 cm^{-1}, respectively, due to a hydrogen-bonded hydroxy group,[13a], while a sharp absorbance at 3600–3640 cm^{-1} arising from a free hydroxy group[13a] is absent. According to a $\Delta\nu_{OH}$-based estimation of the strength of the intramolecular hydrogen bond,[13a] the detected hydrogen bonds belong to a strong OH···N type bond.[13b,c]

The difference between the chemical shifts (0.4 ppm) of the bridgehead protons of tropinone (**11**) and its derivative **16** shows the shielding influence of the magnetic anisotropy of the phenyl groups on the equatorial α-substituents of the piperidine ring for compounds of this type. Hence, we can assign the substantially downfield singlets of the α-methyl substituents for **5**–**7**, **15**, **17**, and **19** (see, e.g., Table 1) to

0947-6539/02/0813-3018 $ 17.50+.50/0 *Chem. Eur. J.* **2002**, *8*, No. 13

equatorial methyl groups. We can also conclude that these methyl groups and the phenyl fragments of the *N*-substituent are spatially proximal (the one downfield signal among the signals of the α-methyl groups for **5** and **15** indicates the spatial proximity of the phenyl group to one of the equatorial methyl groups). These experimental data together with those related to the hydrogen bonds are complementary to the calculation results which rigorously relate the lowest energy conformer for piperidines **5**–**7**, **15**, **17**, and **19** to conformer **A** (see Figures 2 and Scheme 3 as well as the section on molecular mechanics calculations).

Figure 2. Calculated geometry of selected low energy chair conformers for piperidines **4** and **5**. Top: the lowest energy conformer of **4** by MM3; middle: the lowest energy hydrogen-bonded conformer of **5** by MM3 (**A′**); bottom: the lowest energy conformer of **5** by OPLS as well as Amber force fields (**A**). An intramolecular hydrogen bond is present in the middle and bottom chairs.

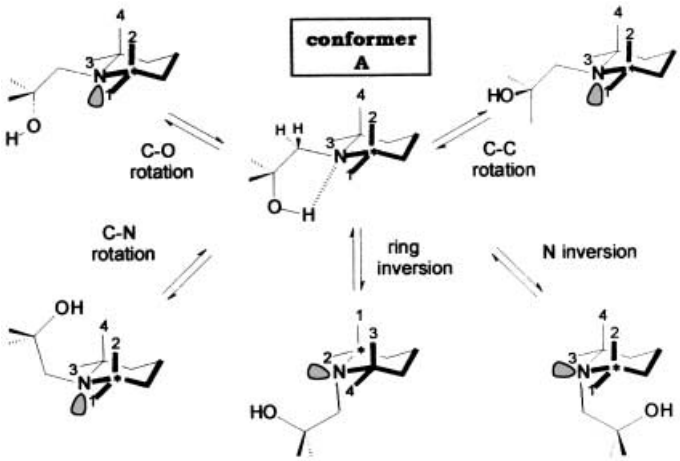

Scheme 3. Each of the five isolated intramolecular dynamic processes results in the break-up of the intramolecular hydrogen bond in conformation **A** of *N*-(2-hydroxyethyl)piperidines (the asterisk is a formal label, numbers indicate the methyl groups).

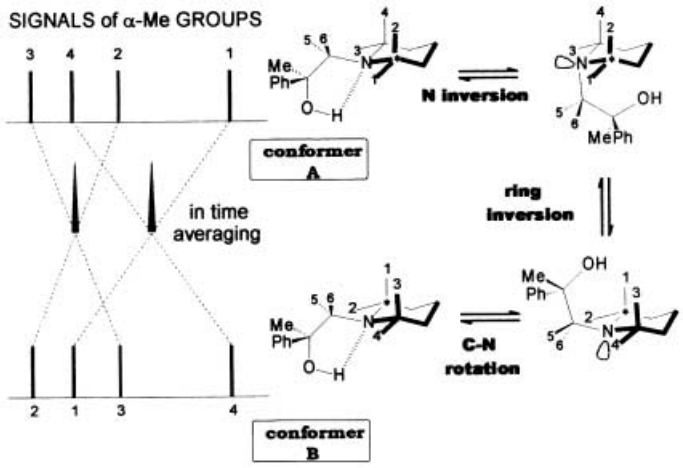

Figure 3. Manifestation of fast topomerization with the temperature increase in the NMR spectra of piperidine **6**. Chair **A** ↔ chair **B** topomerization is shown schematically by three formal intramolecular motions. The ring methyl groups are indicated by numbers 1–4 while numbers 5 and 6 correspond to the *N*-CH_2 protons (the asterisk is a formal label).

Topomerization kinetics: Four signals are seen for the geminal methyl groups in the room-temperature NMR spectra of piperidines **1e**,[5] **6**, and **15** (this work), which possess a chiral ring substituent. These collapse into two at higher temperatures (0.74 and 1.01 ppm at 427 K for **6**). The equally oriented Me groups on opposite sides of the ring (1/3 and 2/4, see Figure 3), and the geminal ring substituents (Me groups 1/2 and 3/4) remain anisochronous under conformation transformations of these piperidines. In contrast, diastereotopomerization occurs for the pair of Me groups 1/4 (and 2/3) of different (axial or equatorial) orientation, for example, in compound **6**. Thus, the averaging in time equalizes two pairs of the four nonequivalent Me groups for **1e**,[5] **6**, and **15**. When the molecule does not possess a chiral center (as in **4**, **5**, and **7**), two pairs of geminal Me substituents (two axial and two equatorial) become equal under the conditions of fast conformation exchange.

The difference in resonance frequency for the two N-CH_2 protons in compounds **1e** and **6** is temperature-independent (see ref. [5] for **1e** and this work for **6**). Lowest energy conformers **A** and **B** (see Figure 3) of piperidine **6** are both identical in energy and also the sole populated conformations (see section on molecular mechanics calculations). Therefore, the chemical shift differences for the N-CH_2 protons as well as for two pairs of the α-methyl groups for **1e** and **6** represent the values of intrinsic anisochronism for these substituents.

The activation parameters for the intramolecular motion in **4**–**7** were obtained by iterative fitting of the signals of the α-methyl groups of the piperidine ring to their simulated line

Table 3. Kinetic parameters for the topomerization of geminal substituents in piperidines **4**–**7**.

T [K]	**4**		**5**		**6**		**7**	
	k [s^{-1}]	$\Delta G^{\neq}$ [kcal mol^{-1}]	k [s^{-1}]	$\Delta G^{\neq}$ [kcal mol^{-1}]	k [s^{-1}]	$\Delta G^{\neq}$ [kcal mol^{-1}]	k [s^{-1}]	$\Delta G^{\neq}$ [kcal mol^{-1}]
235.6	25 ± 4	12.2 ± 0.2						
256.2	180 ± 20	12.3 ± 0.1						
276.9	550 ± 120	12.6 ± 0.2						
301.7	6700 ± 2000	12.4 ± 0.2						
303.6							3.5 ± 1	17.1 ± 0.2
313.9							11 ± 2	16.9 ± 0.1
324.2							32 ± 4	16.8 ± 0.1
334.5			5.5 ± 0.5	18.5 ± 0.2			78 ± 20	16.8 ± 0.1
344.7			10.5 ± 1	18.7 ± 0.2	8 ± 2	18.9 ± 0.2	160 ± 40	16.8 ± 0.2
355.0			26 ± 3	18.6 ± 0.1			600 ± 170	16.4 ± 0.2
365.3			84 ± 20	18.3 ± 0.1	21 ± 3	19.3 ± 0.1	2400 ± 900	15.9 ± 0.3
381.0			220 ± 40	18.4 ± 0.1	70 ± 8	19.3 ± 0.1		
396.2			800 ± 150	18.2 ± 0.2	240 ± 40	19.1 ± 0.1		
411.6					600 ± 100	19.2 ± 0.2		
427.0					1500 ± 300	19.1 ± 0.2		

shapes (^{13}C for compound **4** and ^{1}H for compounds **5**–**7**). The results obtained (see Table 3) show only weak dependence of the free energy of activation ($\Delta G^{\neq}$) on the temperature for most of the studied compounds (as is the case for piperidines **1a** and **1b**[4]). We can, therefore, compare $\Delta G^{\neq}$ values for these compounds with that of steric energy difference (ΔE; see below), obtained from molecular mechanics calulations, even though the force field parameterization does not accurately take into account the entropy contribution.

We can conclude that an increase in the crowding of the amino fragment (a combination of β-branching of the *N*-substituent with complete substitution of the α-positions of the piperidine ring) leads to increase of these barriers. Indeed, among piperidines **1b**, **4**, and **7** (amines without an intramolecular OH···N bond) the difference between $\Delta G^{\neq}$ values for the *N*-Et compound **1b**[4] and *N*-isoBu compound **4** is 1.8 kcal mol^{-1}, while that between compounds **4** and the more hindered **7** is 4.3 kcal mol^{-1}. It is also possible to estimate the contribution of an intramolecular hydrogen bond to the barriers for hindered *N*-(2-hydroxyethyl)piperidines. The lowest energy conformer of **5** is stabilized by the OH···N bond by 1.8 kcal mol^{-1} relative to the related acetate **7** (the difference between the barrier values for close analogues **5** and **7**). Thus, the presence of this bond causes an increase in the barrier approximately by an additional 2 kcal mol^{-1}. This energy estimate is in excellent agreement with experimental values for piperidines **5** and **24**; while the $\Delta\nu_{OH}$ value for **5** is about 340 nm, the intramolecular OH···N bond with ΔG^{0} of 1.8 kcal mol^{-1} for **24** is characterized by a $\Delta\nu_{OH}$ value of 347 nm.[14]

In a similar fashion to piperidines **5**–**7**, the topomerization process is so slow for hindered piperidones **15**, **17**, and **19** as to provide separation of the signals of the geminal ring substituents for **15** and **17** in the room-temperature NMR spectra; for the *trans*-isomer of **19**, this applies to all the substituents. This is not only because of the increase in the bulk of the *N*-substituent (even with intramolecular hydrogen bonding). As with *N*-Me compound **13**, no signal doubling is observed for the geminal ring protons in the room temperature ^{1}H NMR spectrum of piperidone **18**.

Molecular mechanics calculations and barrier assignment

The assignment of the NMR-measured barriers to specific intramolecular dynamic process(-es) is not straightforward for compounds with complex conformation dynamics, for example, for amines.[4, 15, 16] A rational approach for organic systems consists of computational modeling of their potential energy hypersurface. Comparison with the calculated barriers evidently permits determination of the lowest energy conformation pathways and thus to assignment of the NMR-measured barriers to the intramolecular dynamic processes that constitute the highest energy points in these pathways. For organic molecules with a low number of atoms, the strategy may consist of an energy calculation for a relatively low number of all the stationary points forming the conformation graph of an assumed structure.[17, 18] However, knowledge about the number of these points and the formal relationship between them is limited already in the case of five- or six-membered rings.[3, 4]

In addition, concerted processes have often been overlooked in such modeling. For instance, experimental barriers for heterocycles **3a** and **3b** have been assigned to the corresponding pseudorotation transition states[6c] using the conformation scheme for cyclohexane[19] as the source of a set of stationary points. Hence, the low-energy topomerization itineraries for these six-membered cycles are screened according to a "common" stereodynamic model (for cyclohexane[19]), while, as mentioned above (see Introduction), conformation dynamics may be different even for related compounds. The conformation schemes for cyclohexane and piperidines are not the same.[3, 4] As a result, the study of **3a** and **3b**[6c] is not very useful in determining possible conformation itineraries for topomerization of the geminal substituents. Therefore, in spite of intensive use of calculations, the assignment[6c] of the experimental barriers for piperidine **3a** and related morpholine **3b** to the pseudorotation transition states is unreliable. An appreciable deviation of the calculated barriers from the experimental values ($\approx$2 kcal mol^{-1} of overestimation) backs up our suspicion.

More reliable computational modeling of conformation dynamics consists of the generation of a conformational space

  0947-6539/02/0813-3020 $ 17.50+.50/0 *Chem. Eur. J.* **2002**, *8*, No. 13

by different heuristic methods.[20a–g] Recently, a reliable MM3-based approach has been developed for organic compounds of relatively simple structure.[3, 4, 20i,j] Full conformation schemes are created by using the MM3 package[21a–c] without preliminary assumptions. This allows assignment of the experimental barriers for compounds with complex stereodynamics.[3, 4]

This MM3-based methodology[3, 4] is employed here for compound **4**. The full conformation scheme (Figure 4) was built by the MM3-assisted stochastic conformation search (for details see Experimental Section). This finds the conformations, some of which correspond to energy minima (stable conformers) and others correspond to energy maxima (transition states, which are distinguished from the stable conformers by means of the normal mode vibrational analysis included in MM3). Conformations with $\Delta E > 16$ kcal mol^{-1} (relative to the lowest energy conformer) are not included in the scheme, since they are significantly higher than the experimental barrier for **4**. Formal relationships between the transition states and corresponding stable conformers were established by energy minimization for intermediate structures that lie between the transition state and the corresponding stable conformers. These structures were obtained using the Vibplot program (a MM3 package component) using the eigenvectors for the transition states.

Stable conformers: As expected, the lowest energy stable conformers for piperidines **4**–**7** adopt a chair form of the piperidine ring according to the MM3 package-based stochastic search. The Monte-Carlo conformation search implemented within the Macromodel package[22a–c] with MM3* (a slightly modified MM3 force field; Macromodel package), OPLS and Amber force fields inside the Macromodel package (for details see Experimental Section) confirm this conclusion, for example, for compounds **5** and **6**. In addition, for the chair conformers of **4**–**7** and **17** the endocyclic C–N bonds and the C_α–H bonds of the *N*-substituent (see Figure 2) are eclipsed. Thus, amines **4**–**7**, **15**, **17**, and **19** belong to a rare set of alkylamines for which isolated nitrogen inversion[4] (INI) is possible owing to eclipsing in the stable conformers.[4]

The experimentally detected predominance of a conformation with an intramolecular OH···N bond for aminoalcohols **5**, **6**, and **15**–**19** (see section on NMR and IR spectroscopy) is not reproduced well by MM3. For compound **5**, this is probably because of insufficiently good parameters for hydrogen bonds in this generally reliable force field. An MM3-based stochastic search for **5** by using the hydrogen-bond parameters of MM3 identified the three lowest energy conformers as similar chairs with different locations of the OH group proton. The difference in steric energy ΔE for these conformers is 0, 0.3, and 0.3 kcal mol^{-1} and only one among the two last conformations is intramolecularly hydrogen-bonded (**A′** in Figure 2). However, the Amber and OPLS force fields, with better parameters for hydrogen bonds, recognize chair **A** with an intramolecular OH···N bond as the strongly predominant conformation for **5**. A Monte-Carlo-based conformation search with these force fields found this conformer to be the lowest in energy and, in addition, to be the only conformer within a 3 kcal mol^{-1} ΔE range. Also for aminoalcohols **16** and **25**, only intramolecularly hydrogen-bonded conformers (more than ten for **16** or **25** within a 2 kcal mol^{-1} ΔE range) were identified by these force fields as the lowest energy conformers.

Conformation dynamics: Seven intramolecular dynamic processes are possible for N-Et compound **1b** (excluding rotation of the methyl groups):

isolated C–N rotation (ISR), nitrogen inversion/rotation (NIR), ring inversion (RI), ring inversion/nitrogen inversion (RINI), ring inversion/C–N rotation (RIR), ring inversion/nitrogen inversion/C–N rotation (RINIR), isolated nitrogen inversion (INI).

Six of these (see Figure 4), as well as additional rotations around the C–C bond and a concerted rotation around the C–C and C–N bonds of the isoBu substituent, are present for piperidine **4**. The generated conformations of **4** may be classified into two equal groups ((*l*) and (*d*)-diastereotopomers in Figure 4) according to diastereotopic relations between the geminal substituents of the piperidine ring. For instance, chairs $\mathbf{A_1}$ and $\mathbf{A_2}$ with equatorial methyl substituents 1 and 3 belong to the group of (*l*)-diastereotopomers", while chairs $\mathbf{B_2}$ and $\mathbf{B_1}$ with axial orientation of these substituents belong to group (*d*)diastereotopomers. Only part of the group of (*d*)-diastereotopomers is represented in order to avoid overloading the scheme.

Formal transition from one group to another is necessary in order to provide the NMR-observed topomerization (e.g., $\mathbf{A_1} \leftrightarrow \mathbf{B_2}$). Two pathways ($L_1$ and L_2) of the topomerization (with the high-energy points being a chair and a 1,4-half-chair with $\Delta E = 12.0$ and 12.3 kcal mol^{-1}, respectively) are appreciably lower in energy than all others. The high-energy points for L_1 correspond to RI (4-sofa with $\Delta E = 12.0$ kcal mol^{-1}) and a concerted C–N/C–C rotation of the *N*-substituent (chair with $\Delta E = 12.0$ kcal mol^{-1}). For L_2 these points correspond to RINI (1,4-half-chair with a planar nitrogen fragment; $\Delta E =$ 12.3 kcal mol^{-1}) and a concerted C–N/C–C rotation of the *N*-substituent (chair; $\Delta E = 12.0$ kcal mol^{-1}). Since the energy difference between the high-energy points is small for the lowest energy itineraries L_1 and L_2 (0.3 kcal mol^{-1}), as well as for the points for L_2 (0.3 kcal mol^{-1}), the measured barrier should be assigned to simultaneous slowing of RI, RINI, and concerted C–N/C–C rotation.

These calculations are in very good agreement with the DNMR measurements (Table 4; the averaged experimental $\Delta G^{\neq}$ value for **4** is given): the deviation of the calculated barriers from the experimental one is only 0.1–0.4 kcal mol^{-1}. We emphasize that, as for other examples,[3, 4] the similarity of the measured topomerization barrier to the calculated values *in the topomerization-providing itineraries of lowest energy* strongly supports the conformation scheme for piperidine **4**.

Table 4. Calculated[a] and experimental values [kcal mol^{-1}] of the barriers for piperidine **4**.

ΔE for conformation pathway L_1	ΔE for conformation pathway L_2	Averaged experimental $\Delta G^{\neq}$ value
12.0 (RI)	12.3 (RINI)	12.4
12.0 (ISR-ISR)	12.0 (ISR-ISR)	

[a] Relative to the lowest energy conformer.

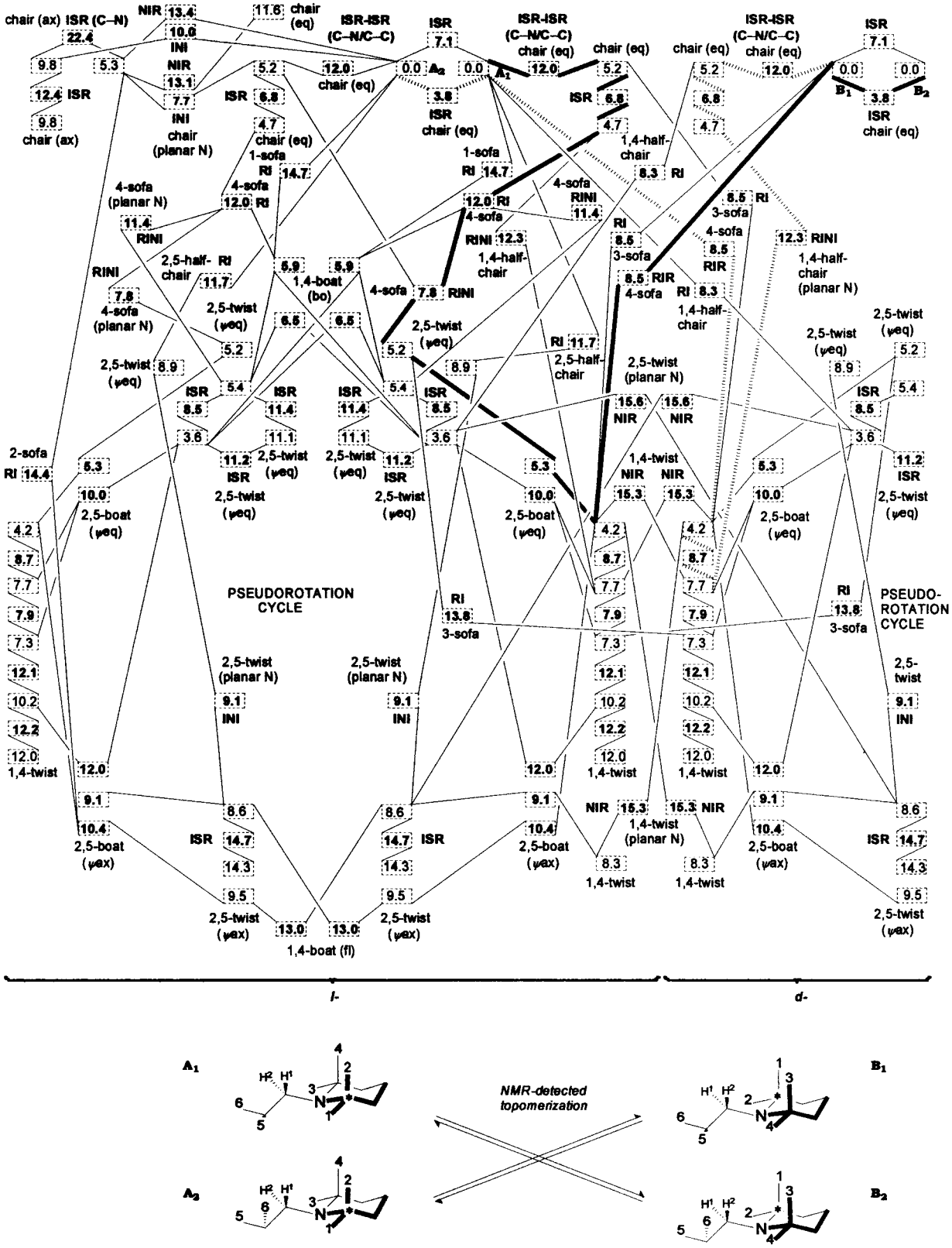

Figure 4. Scheme of conformation transformations for piperidine **4** (only a representative part of the scheme, fragment (*l*), is shown). Energies (in rectangles, kcal mol^{-1}) are relative to the lowest energy conformer. The asterisk is a formal label, numbers indicate the methyl groups. Conformers of the same ring geometry are grouped in columns. The names and the relative energies for the transition states are in bold (transition states in a 1,4-twist ring conformation belong to ISR). The orientation of the *N*-substituent is shown in parentheses (ax: axial, eq: equatorial, ψeq: pseudoequatorial, ψax: pseudoaxial, bo: bowsprit, fl: flagstaff). Chair $\mathbf{A_1} \leftrightarrow$ chair $\mathbf{B_2}$ itinerary L_1 of low energy is marked by bold lines. Another low energy chair $\mathbf{A_2} \leftrightarrow$ chair $\mathbf{B_1}$ pathway L_2 is shown by dotted lines.

  0947-6539/02/0813-3022 $ 17.50+.50/0 *Chem. Eur. J.* **2002**, *8*, No. 13

Thus, the same three dynamic processes are slowest in the topomerization of piperidine **4**, with a branched *N*-substituent (RI, RINI, and ISR/ISR), and for piperidines **1b–d**, with a primary *N*-alkyl substituent (RI, RINI, and ISR, see Introduction). Participation of RI and RINI is quite an unexpected result for **4**; experimental barriers for these processes are appreciably lower, for example, for the parent compound **1a**.[4] Lower energy RI and RINI transition states are also present for **4** (a 3-sofa with $\Delta E = 8.5$ kcal mol^{-1} or a 4-sofa with $\Delta E = 8.3$ kcal mol^{-1}). However, the conformation scheme shows that among the RI and RINI transition states of **4** the high energy ones lie in the lowest energy itineraries L_1 and L_2.

In spite of the similarity in conformation dynamics for piperidines with primary and with β-branched *N*-substituents, we would prefer not to extrapolate the above conclusions for **4** to the more hindered compounds **5–7**, **15**, **17–19** because of the lack of reliability of a such an assignment (see Introduction). Only ISR may be also attributed to compounds **5–7**, **15**, **17–19** as a rate-determining intramolecular dynamic process; an increase of rotation-associated barriers usually correlates with an increase of steric hindrance of the rotating fragment[15, 23, 24] (see ref. [25] for an exception). In principle, the NIR barrier also increases with the crowding of the nitrogen fragment for some sterically-encumbered amines (we singled out these amines as a third type of alkylamines[24]). Nevertheless, NIR is not involved in the observed slowing of the topomerization in the studied piperidine derivatives. The calculated values of the lowest ISR and NIR barriers (by MM3) for piperidine **7** in chair conformation **A** are 16.1 and 13.0 kcal mol^{-1}, respectively: only the calculated ISR barrier is close to the experimental value (the averaged $\Delta G^{\neq}$ value is 16.7 kcal mol^{-1}). It is remarkable that the measured barrier for hindered amine **6**—19.2 kcal mol^{-1}—is the highest barrier known as yet for rotation around a C–N bond in aliphatic amines.

Hydrogen-bonded amines and NIR

An acyclic analogue of *N*-(2-hydroxyethyl)piperidines (e.g., **18**) is amine **25** (see Figure 1). Topomerization of methyl groups for this compound (a formal result of subsequent NIR and ISR) in acidic water solution has been detected by DNMR spectroscopy.[26a] However, we accept neither the value quoted for the "apparent barrier" nor the assignment of the measured barrier to nitrogen inversion.

The 8.8 kcal mol^{-1} value extracted from the DNMR data (given by the authors[26a] as the nitrogen-inversion barrier) would only be significant if "the rate of interconversion of amine and salt is rapid"[27] in acidic solution. However, the deprotonation of the ammonium salt is not rapid, and it can be significantly slower than pyramidal inversion in alkylamines. Free energies of activation for deprotonation in alkylamines[28a,b] lie in the range 15–17 kcal mol^{-1}, while the NIR barriers do not usually exceed the 9–10 kcal mol^{-1} limit (see refs. [3, 15, 16] for values of NIR in amines and ref. [24] for structural features of exceptional alkylamines, such as amine **4**, possessing high NIR barriers). The barriers for dissociation of an intermolecular hydrogen bond in simple aliphatic amines in water (i.e., for a HOH$\cdots$NR$_3$ form) are also not high (lower by 4–5 kcal mol^{-1}).[28a,b] Thus, the required deprotonation step is rate-determining for the observed diastereotopomerization of **25** in acidic solutions (see Scheme 4; indicated as a kinetic stage with constant k_a also

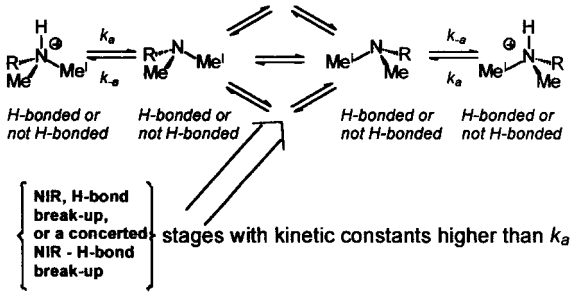

Scheme 4. Simplified scheme of diastereotopomerization of the *N*-Me groups in amine **25** in acidic solutions (spatial reorganization of substituent R is not considered). Deprotonation with kinetic constant k_a is the rate-determining step of this topomerization.

in ref. [28a,b]), and the authors[26a] actually measured k_a under different conditions (as k_{obs} in ref. [26]) and not a NIR barrier. Unfortunately, the use of this inadequate kinetic model[27] led to the similarly incorrect assignment to nitrogen inversion for tens of alkylamines (reviewed in refs. [2b, 15]).

Another study in the literature[26b] measured that a barrier of 16.3 kcal mol^{-1} for the diastereotopomerization of the methyl groups (their signals coalesce above room temperature) of the protonated form of the antidepressant drug **26** (Figure 1). Pyramidal nitrogen inversion is carefully discussed only as a process that provides isochronism for the *N*-Me groups, but the authors do not link the experimental barrier and the deprotonation process for the ammonium salt of **26**, even though this is the rate that was in fact measured.

The claim that in aminoalcohol **25** "the hydroxy proton does not reach the nitrogen to form a hydrogen bond", is an additional problematic point.[26a] In the light of our experimental data for the above piperidine derivatives (see section on NMR and IR spectroscopy) as well as the above calculation results for **25**, a strong intramolecular OH$\cdots$N bond should be present in **25** in aprotic nonpolar solutions. In water, the only question is whether the amine is intermolecularly or intramolecularly hydrogen bonded. Thus, the assignment[26a] of the NMR-detected conformation transformation to nitrogen inversion would be unreliable even in the hypothetical case of fast deprotonation kinetics. Without an adequate quantitative conformation scheme one may not conclude for which process the rate has been measured in the case of aminoalcohol **25**: NIR, ISR, a concerted hydrogen bond dissociation/NIR or a concerted H-bond dissociation/ISR process. Finally, to consider the obtained value[26a] as "typical" for the conformation dynamics of *N*,*N*-dimethyl-*N*-alkyl amines is incorrect. The NIR barrier for an amine strongly depends on the structure of the *N*-alkyl substituent.[24, 25] For example, the NIR barrier for Me_3N[29] is 8.2 kcal mol^{-1}, while for *N*,*N*-dimethyltriptycylamine it is too low[24, 29] to be measured by conventional DNMR techniques.

In general, the literature does not discuss how NIR or ISR occur for hydrogen-bonded amines (such as alkylamines possessing an intramolecular OH···N bond), whether stepwise, through a break-up of the hydrogen bond followed by NIR or ISR in the intermediate free amine, or as a synchronous process of NIR or ISR and hydrogen-bond dissociation. For instance, a description of conformation dynamics for *N*,*N*-diethylaminomethylphenols with an intramolecular OH···N bond[30a,b] presumes only a two-step mechanism for NIR: break-up of the chemical bond (hydrogen bond) followed by the usual conformation transformation of a free amino group (NIR). Other topomerization mechanisms for amines in aqueous solutions are actually intermolecular and do not include pyramidal nitrogen inversion itself.[30c]

We analyzed whether there is a NIR transition state that is a single energy maximum in the pathway hydrogen-bonded invertomer 1 to non-hydrogen-bonded invertomer 2 using MM3-based modeling. Several first-order NIR transition states for piperidine **5** were generated (see Experimental Section for details) and their relationship with the corresponding stable conformers was established as described above. Indeed, two transition states (TS_1 and TS_2; see Figure 5) for a concerted hydrogen-bond dissociation/NIR process were found. The lowest energy hydrogen-bonded chair with an equatorial *N*-substituent (conformer ***A′***; see also Figure 2) and the lowest energy hydrogen-bonded chair with an axial *N*-substituent are transformed through the corresponding transition states into non-hydrogen-bonded chairs with an axial and equatorial substituent, respectively.

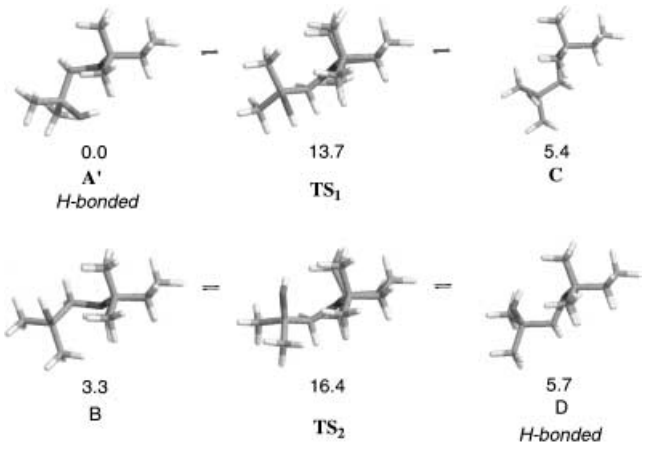

Figure 5. Two NIR transition states (TS_1 and TS_2) and the corresponding stable conformers for piperidine **5** (MM3-optimized structures are presented). Energies (kcal mol^{-1}) are shown as relative values to steric energy of conformer **A′**.

Since MM3 does not provide the desired accuracy in the energy calculation for hydrogen-bond-containing conformers (see above) the Amber force field was also employed to check the MM3 results. The relationship between TS_1 and the corresponding conformers **A** and **C** for amine **5** was established similarly to the MM3 case, by using full-matrix minimization and the normal mode vibrational analysis implemented by Macromodel. It was found that TS_1 (optimized by Amber) for NIR in piperidine **5** lies between conformers **A** (hydrogen-bonded; see Figure 2) and **C** (not hydrogen-bonded; Figure 5) in the pathway **A** ⇌ **C**.

Finally, we undertook quantum mechanical ab initio calculations in order to examine these conformation transformations (e.g., **B** ⇌ **D**) by a reliable and independent method. Optimization of the MM3-derived geometry of TS_2 at the RHF/6-31G* level led to a first-order transition state of essentially the same geometry as that obtained by the molecular mechanics force fields. As in the case of molecular mechanics, normal mode vibrational analysis (carried out using Gaussian98[31]) demonstrated that this TS_2 is the transition state for the conformation transformation of non-hydrogen-bonded conformer **B** into hydrogen-bonded **D** and vice versa. This confirms our hypothesis of a concerted hydrogen bond dissociation-NIR process taking place in hydrogen-bonded amines.

Experimental Section

Acetonitrile and triethylamine were dried and distilled, while other analytical grade solvents and commercial reagents (Aldrich) were used without additional purification. Piperidine derivatives **8**, **11**, and **13** are commercially available (piperidone **13** was redistilled before use). Piperidones **12** and **14** (a 1:1 mixture of *cis*- and *trans*-isomers) as well as piperidol **22** were obtained according to the reported procedures.[1b, 32, 33] An Osram 125 W medium-pressure lamp was used as an external UV light source. Elemental analysis was carried out for compounds **15**–**19**; for related compounds **4**–**7** high-resolution mass spectra were obtained and the purity was ascertained by TLC in two different systems ($CHCl_3$/EtOH, 15:1 and $CHCl_3$/diethyl ether, 2:1) on silica gel 60 F_{254} plates (Merck) and in one chromatography system (MeCN/water, 9:1) on KC18 reversed silica plates (Carlo Erba Reagenti). High-resolution mass spectra (chemical ionisation, reagent gas isobutane) were recorded on a VG AutoSpec mass spectrometer; other mass-spectra were recorded on a VG-7070E spectrometer (70 eV, 50–100°). IR spectra were obtained for 0.001–0.0005 M solutions of piperidine compounds in dry CCl_4 on a Perkin–Elmer 580B instrument.

All ^{1}H and ^{13}C NMR spectra were obtained on a Bruker AM-300 spectrometer. TMS was used as internal standard. Samples (20–30 mg in C_6D_5Br (0.5 mL)) were equilibrated ≈10 min at each temperature before every NMR experiment. Temperatures were measured with a calibrated Eurotherm 840/T digital thermometer and are believed to be accurate to ±0.5 K. For the complete line-shape analysis, a modified version of a program written by R. E. D. McClung, University of Alberta, Edmonton (Canada), was used with visual fitting. At the lowest measured temperature the $\Delta\delta$ values were 1109 Hz (**4**, ^{13}C), 36.4 Hz (**5**, ^{1}H), 53.6 and 121.7 Hz (**6**, ^{1}H, two pairs of methyl singlets) and 21.8 Hz (**7**, ^{1}H). In every case, 3–5 $\Delta\delta$ values, at different temperatures, were obtained from the fitting procedure. These were extrapolated for the calculated line shapes at temperatures above coalescence. The contributions to the linewidth from the dynamic process were 1 Hz or more (at the lowest and/or highest temperature extremes) for the entries in Table 3. The activation parameters were calculated by using the Eyring equation.

The 1996 version of the MM3 program[21a–c] with an explicit parameters for amines[21b] was used for molecular mechanics calculations. Energy minimization in the regions of the minima and maxima of steric energy was performed without restriction for the structural elements (full-matrix minimization option). For the calculation of barriers in **5** and **7**, two procedures were employed: a) the dihedral driver option and b) the one-plane fixation of the *N*-fragment. In a), the exocyclic *N*-substituent was rotated in the range −180 to +180° around both the C–N and C–N bonds (NDRIVE = −1; block diagonal minimization; 6° rotation steps for each dihedral angle). In the regions of the energy maxima 1° rotation steps were used. Full-matrix minimization (option 3) was further used for the high-energy points. For b), amine structures with a planar amino fragment were

  0947-6539/02/0813-3024 $ 17.50+.50/0 *Chem. Eur. J.* **2002**, *8*, No. 13

oriented to place the N atom and the two ring C_α atoms in the *xy* plane; the *z* coordinate of the third C_α atom was changed to zero. Block diagonal minimization of this structure with restricted motion along the *z* coordinate for the N atom and three C_α atoms was performed; the final step was full-matrix minimization (option 3) for the resulting structures. In both cases a) and b) the NIR transition states were distinguished from the ISR transition states by normal mode vibrational analysis.

A stochastic search followed by full-matrix minimization (option 9) was used for the generation of an entire set of transition states and stable conformations for piperidine **4**. This search (200 pushes) was performed six times, starting from different ring conformations until no new conformations were generated in the last search. Coordinates derived from the eigenvectors (produced by option 5 and Vibplot) of vibrational modes with imaginary frequency were employed as starting coordinates for minimization in the establishment of the formal relationship between conformers and transition states.

MM3*, Amber and OPLS force fields (Macromodel 6.5 package[22a–c]) were used for conformation analysis of the piperidine compounds as well as amine **25**. The "no solvent" and "distance-dependent dielectric electrostatics" options were employed for the energy minimization. Full-matrix minimization (FMNR) and vibrational analysis (VIBR) options were used in the case of the NIR transition state for piperidine **5**. The "Monte-Carlo" option was used for conformation search (generation of 5×10^5 structures for each compound with the energy upper limit 3 kcal mol^{-1} from the lowest energy conformer found).

The Gaussian 98 package[31] was used for ab initio calculations (gas phase) of the transition state of a concerted NIR/hydrogen-bond dissociation process in **5** by employing the Berny optimization algorithm and the Newton–Raphson optimization procedure at each level of ab initio calculations. MM3-derived geometry for TS_2 served as the starting structure. Initial ab initio geometry optimization was performed at the restricted Hartree–Fock level with the 3-21G basis set. The resulting geometry was optimized at the RHF/6-31G* level. For the location of the first-order NIR transition states the "NoEigenTest" option was employed at the initial calculation step at the RHF/3-21G level, followed by the use of the "CalcAll" option in the next calculation step (at the same level of theory). Further calculations with the "CalcAll" option were carried out at the RHF/6-31G* level.

General procedure for preparation of piperidines 5, 6, 15–19: A solution of amine **2** (10 mmol) in a benzene/ketone **10a** mixture (7:3, 100 mL) or a solution of amines **2** or **12** (10 mmol) and ketone **10b** (15 mmol) in benzene or a solution of amines **11–14** (10 mmol) and ketone **10c** (15 mmol) in benzene (80–100 mL) in a quartz flask were irradiated under reflux with bubbling argon for 10–15 h. A solution of H_2SO_4 (10 mmol) in water (50 mL) was added, the aqueous phase treated with NaOH to pH ≈ 12 and extracted with $CHCl_3$, and the organic layer evaporated and purifies by chromatography on a silica column. Gradient elution (from CCl_4 to $CHCl_3$) afforded compounds **5**, **6**, **15–19**.

1-(2-Hydroxy-2-phenylpropyl)-2,2,6,6-pentamethyl-4-piperidone (15): M.p. 83–84 °C; IR (CCl_4): $\tilde{\nu}$ = 1720 (C=O), 3260 cm^{-1} (OH); elemental analysis calcd (%) for $C_{18}H_{27}NO_2$ (289): C 74.7, H 9.3, N 4.8; found: C 74.4, H 9.3, N 5.0.

8-(2-Hydroxy-2,2-diphenylethyl)-8-azabicyclo[3.2.1]octane-3-one (16): M.p. 106–108 °C; ^{1}H NMR ($CDCl_3$): δ = 1,49 (m, 2H; *H*-6, *H*-7), 1.88 (m, 2H; *H*-6, *H*-7), 2.04 (dd, ^2J(H,H) = 16.5 Hz, ^3J(H,H) = 1.5 Hz, 2H; H_{ax}-2, H_{ax}-4), 2.50 (dd, ^2J(H,H) = 16.5 Hz, ^3J(H,H) = 4.5 Hz, 2H; H_{eq}-2, H_{eq}-4), 3.40 (s, 2H; *N*-CH_2), 5.4 (br s, 1H; OH), 7.2–7.8 (m, 10H; Ph); IR (CCl_4): $\tilde{\nu}$ = 1710 (C=O), 3372 cm^{-1} (OH); MS: *m*/*z* (%): 303 [$M^+ - H_2O$]; elemental analysis calcd (%) for $C_{21}H_{23}NO_2$ (321): C 78.5, H 7.2, N 4.5; found: C 78.3, H 7.4, N 4.5.

1-(2-Hydroxy-2,2-diphenylethyl)-2,2,6,6-pentamethyl-4-piperidone (17): M.p. 216–218 °C; ^{1}H NMR ($CDCl_3$): δ = 0.7 (s, 6H; α-Me_{eq}), 1.01 (s, 6H; α-Me_{ax}), 2.00 (d, ^2J(H,H) = 11.5 Hz, 2H; H_{ax}-3, H_{ax}-5), 2.48 (d, ^2J(H,H) = 11.5 Hz, 2H; H_{eq}-3, H_{eq}-5), 3.54 (s, 2H; *N*-CH_2), 5.5 (br s, 1H; OH), 6.9–7.6 (m, 10H; Ph); IR (CCl_4): $\tilde{\nu}$ = 1725 (C=O), 3360 cm^{-1} (OH); elemental analysis calcd (%) for $C_{23}H_{29}NO_2$ (351): C 78.6, H 8.3, N 4.0; found: C 78.6, H 8.1, N 3.1.

1-(2-Hydroxy-2,2-diphenylethyl)-4-piperidone (18): M.p. 62–64 °C; ^{1}H NMR ($CDCl_3$): δ = 2.28 (t, ^3J(H,H) = 6.0 Hz, 4H; β-H), 2.67 (t, ^3J(H,H) = 6.0 Hz, 4H; α-H), 3.38 (s, 2H; *N*-CH_2), 5.2 (br s, 1H; OH), 7.0–7.7 (m, 10H; Ph); IR (CCl_4): $\tilde{\nu}$ = 1710 (C=O), 3392 cm^{-1} (OH); elemental analysis calcd (%) for $C_{19}H_{21}NO_2$ (295): C 77.3, H 8.6, N 4.7; found: C 77.0, H 8.9, N, 5.1.

1-(2-Hydroxy-2,2-diphenylethyl)-2,2,3,5,6,6-heptamethyl-4-piperidone (a 1:1 mixture of *cis*- and *trans*- isomers) (19): M.p. 127–129 °C; ^{1}H NMR ($CDCl_3$, the signals of the *trans*-isomer are marked by asterisk): δ = 0.57* (s, 3H; α-Me_{eq}), 0.71 (s, 3H; α-Me_{eq}), 0.71* (s, 3H; α-Me_{eq}), 0.78 (s, 3H; α-Me_{ax}), 0.83* (s, 3H; α-Me_{ax}), 0.96* (s, 3H; α-Me_{ax}), 0.84–0.88 (m, 9H; β-Me), 1.24* (d, ^3J(H,H) = 7.2 Hz, 3H; β-Me), 2.14* (q, ^3J(H,H) = 7.2 Hz, 2H; β-H), 2.76 (q, ^3J = 6.6 Hz, 2H; β-H), 3.54* (br s, 2H; *N*-CH_2), 3.62 (s, 2H; *N*-CH_2), 5.4 (br s, 1H; OH), 6.9–8.1 (m, 10H; Ph); IR (CCl_4): $\tilde{\nu}$ = 1716 (C=O), 3400 cm^{-1} (OH); MS: *m*/*z* (%): 361 [$M^+ - H_2O$]; elemental analysis calcd (%) for $C_{25}H_{33}NO_2$ (379): C 79.1, H 8.7, N 3.7; found: C 78.8, H 8.9, N 3.3.

Piperidine 4: A mixture of amine **8** (10 mmol) and iodide **9** (80 mmol) was heated for 4–5 h at 155 °C in a sealed tube. After addition of hexane and filtration the solution was treated with 1 M HCl to pH ≈ 1 and extracted with CH_2Cl_2. The aqueous phase was altered to pH ≈ 11 by using NaOH and extracted with $CHCl_3$. The organic phase was concentrated at 25 °C and loaded on to a 4 cm layer of silica gel. Elution with CH_2Cl_2/diethyl ether (4:1) afforded compound **4**.

1-(2-Acetoxy-2-methylpropyl)-2,2,6,6-tetramethylpiperidine 7: A solution of amine **6** (21 mg, 0.1 mmol), acetyl chloride (24 mg, 0.3 mmol), triethylamine (30 mg, 0.3 mmol), and DMAP (5 mg) in MeCN (2 mL) was stirred for 3 days at 25 °C. Water and CH_2Cl_2 were added, the organic layer evaporated, and gradient chromatography on C_{18} reversed phase silica (from MeCN/water (80:20) to MeCN/water (95:5); eluent volume 200 mL) led to compound **5** (16 mg, 56%).

***N*-Demethylation (general procedure)**: A solution of amine **11**, **12**, or **22** (10 mmol) in a water/ketone **10a** mixture (4:1, 100 mL) was irradiated (quartz) for 8–10 h under reflux and under bubbling argon. H_2SO_4 (0.5 mL), K_2SO_4 (5 g), and $CHCl_3$ (80 mL) were added, the aqueous phase was treated at 0 °C with NaOH to pH ≈ 11 and extracted with $CHCl_3$ (3 × 80 mL), and the organic phase (dried over K_2CO_3) was concentrated. Chromatography on silica led to compounds **20**, **21**, or **23**, respectively.

Acknowledgemments

We are very grateful to a group of professors from the Israeli universities, initiators of the governmental KAMEA support program (Profs. Benjamin Fein, Eliezer Giladi, Dan Amir, Daniel Hupert, Elisha Haas, and others), for their insistent and generous efforts in the ratification and continuation of the program. A Bar-Ilan University grant to A.M.B. is also acknowledged.

[1] a) R. F. Francis, E. L. Colling, *J. Org. Chem.* **1986**, *51*, 1889–1891; b) A. M. Belostotskii, A. B. Shapiro, *Bull. Acad. Sci. USSR Div. Chem. Sci.* **1991**, *40*, 486–495; c) K. Ogawa, J. Harada, M. Endo, Y. Takeuchi, H. Kagawa, *Tetrahedron Lett.* **1997**, *38*, 563–566; d) P. Geneste, J. M. Kamenka, R. Rogues, J. P. DeClercq, G. Germain, *Tetrahedron Lett.* **1981**, *22*, 949–950; e) M. Cygler, M. Markowicz, J. Skolimowski, R. Skowronski, *J. Mol. Struct.* **1980**, *68*, 161–171.

[2] a) T. A. Crabb, A. R. Katritzky, *Adv. Heterocycl. Chem.* **1984**, *36*, 3–176; b) J.-J. Delpuech in *Cyclic Organonitrogen Stereodynamics* (Eds.: J. B. Lambert, Y. Takeuchi), VCH, Weinheim, **1992**, 169–250; c) S. Profeta, Jr., R. J. Unwalla, D. J. Russell, *Int. J. Supercomput. Appl. High Perform. Comput.* **1994**, *8*, 35–46; d) N. S. Prostakov, A. A. Fomichev, N. I. Golovtsov, V. A. Resakov, A. V. Varlamov, *Russ. J. Org. Chem.* **1986**, *21*, 2113–2119; e) F. A. L. Anet, I. Yavari, I. J. Ferguson, A. R. Katritzky, M. Moreno-Manas, M. J. T. Robinson, *J. Chem. Soc. Chem. Commun.* **1976**, 399–400; f) A. M. Belostotskii, A. B. Shapiro, T. V. Timofeeva, Yu. T. Struchkov, *Bull. Acad. Sci. USSR Div. Chem. Science* **1991**, *40*, 77–82.

[3] A. M. Belostotskii, P. Aped, A. Hassner, *J. Mol. Struct. (THEOCHEM)* **1998**, *429*, 265–273.

[4] A. M. Belostotskii, H. E. Gottlieb, P. Aped, A. Hassner, *Chem. Eur. J.* **1999**, *5*, 449–455.

[5] J. E. Anderson, D. Cazarini, J. E. T. Corrie, L. Lunazzi, *J. Chem. Soc. Perkin Trans. 2* **1993**, 1299 – 1304.
[6] a) E. Vilsmaier, W. Tröger, G. Haag, *Chem. Ber.* **1981**, *114*, 67 – 79; b) E. Vilsmaier, J. Fath, G. Maas, *Synthesis* **1991**, 1142 – 1146; c) A. Kolocouris, E. Mikros, N. Kolocouris, *J. Chem. Soc. Perkin Trans. 2* **1998**, 1701 – 1708.
[7] a) S. G. Cohen, A. Parola, *Chem. Rev.* **1973**, *73*, 141 – 161; b) A. M. Belostotskii, L. M. Kostochka, A. P. Skoldinov, *Chem. Heterocycl. Compounds* **1982**, 1280 – 1284.
[8] a) G. Hofle, W. Steglich, *Synthesis* **1972**, 619 – 621; b) A. Hassner, L. Krepski, V. Alexanian, *Tetrahedron* **1978**, *34*, 2069 – 2076.
[9] W. M. Horspool, *Aspects of Organic Photochemistry*, Academic Press, London, **1976**, 163 – 186.
[10] A. Hassner, A. M. Belostotskii, *Tetrahedron Lett.* **1995**, *36*, 1709 – 1712.
[11] J. C. Scaiano, *J. Photochem.* **1973**, *2*, 81 – 118.
[12] H. Möhrle, P. Gundlach, *Arch. Pharm.* **1969**, *302*, 291 – 296.
[13] a) S. A. Aaron, *Top. Stereochem.* **1979**, *11*, 1 – 52; b) It should be noted that the employed classification of the hydrogen bond strength considers only the relative strength of intramolecular hydrogen bonds. For general classification of the strength of different hydrogen bonds seeT. Steiner, *Angew. Chem. Int. Ed.* **2002**, *41*, 48 – 76; c) G. A. Jeffrey, *An Introduction to Hydrogen Bonding*, Oxford University Press, Oxford, **1997**.
[14] K. Kuliñska, M. Wiewiórowski, *Can. J. Chem.* **1987**, *65*, 205 – 212.
[15] J. B Lambert, *Top. Stereochem.* 1971, **6**, 19 – 105.
[16] C. H. Buchweller in *Acyclic Organonitrogen Stereodynamics* (Eds.: J. B. Lambert, E. Takeuchi), VCH, Weinheim **1992**, pp. 1 – 55.
[17] S. A. Glover, A. Rauk, *J. Org. Chem.* **1999**, *64*, 2340 – 2345.
[18] J. Koèa, P. H. J. Carlsen, *J. Mol. Struct. (THEOCHEM)* **1992**, *257*, 105 – 130.
[19] D. Cremer, K. J. Szabo in *Conformational Behavior of Six-Membered Rings* (Ed.: E. Juaristi), VCH, Weinheim **1995**, pp. 59 – 135.
[20] a) H. Gotô, E. Ôsawa, *J. Am. Chem. Soc.* **1989**, *111*, 8950 – 8951; b) S. Fisher, M. Karplus, *Chem. Phys. Lett.* **1992**, *194*, 252 – 261; c) J. Koèa, S. Pérez, A. Imberty, *J. Comput. Chem.* **1995**, *16*, 296 – 310; d) P. Iratcabal, D. Liotard, *J. Am. Chem. Soc.* **1988**, *110*, 4919 – 4926; e) D. D. Beusen, E. F. B. Shands, S. F. Karasek, G. R. Marshall, R. A. Dammkoehler, *J. Mol. Struct. (THEOCHEM)* **1996**, *370*, 157 – 171; f) J. M. Blaney, J. S. Dixon, *Rev. Comput. Chem.* **1994**, *5*, 299 – 335; g) M. Saunders, *J. Comput. Chem.* **1989**, *10*, 203 – 208; h) A. Espinosa, A. Gallo, A. Entrena, J. A. Gomez, *J. Mol. Struct.* **1994**, *326*, 249 – 260; i) A. Espinosa, A. Gallo, A. Entrena, J. Campos, J. F. Dominguez, E. Camacho, *J. Mol. Struct.* **1993**, *296*, 133 – 144.
[21] a) N. L. Allinger, Y. Yuh, J.-H. Lii, *J. Am. Chem. Soc.* **1989** *111*, 8551 – 8582; b) L. R. Schmitz, N. L. Allinger, *J. Am. Chem. Soc.* **1990**, *112*, 8307 – 8315; c) MM3: Available from the Quantum Chemistry Program Exchange, Indiana University, Bloomington, Ind.
[22] a) M. Saunders, K. N. Houk, Y. D. Wu, W. C. Still, M. Lipton, G. Chang, W. C. Guida, *J. Am. Chem. Soc.* **1990**, *112*, 1419 – 1427; c) F. Mohamadi, N. G. Richards, W. C. Guida, R. Liskamp, M. Lipton, C. Caufield, G. Chang, T. Hendrickson, W. C. Still, *J. Comput. Chem.* **1990**, *11*, 440 – 467; c) Macromodel, Version 6.0, Department of Chemistry, Columbia University.
[23] K. Umemoto, K. Ouchi, *Proc. Indian Acad. Sci. Chem. Sci.* **1985**, *94*, 1 – 119.
[24] A. M. Belostotskii, A. Hassner, *J. Phys. Org. Chem.* **1999**, *12*, 659 – 663.
[25] A. M. Belostotskii, H. E. Gottlieb, A. Hassner, *J. Am. Chem. Soc.* **1996**, *118*, 7783 – 7789.
[26] a) H. Santa, R. Laatikainen, S. Lötjönen, P. Palumaa, *J. Chem. Res.* **1992**, 198 – 199; b) J. C. Wilson, S. L. A. Munro, D. J. Craik, *Magn. Reson. Chem.* **1995**, *33*, 367 – 374.
[27] M. Saunders, F. Yamada, *J. Am. Chem. Soc.* **1963**, *85*, 1882.
[28] a) U. Berg, W. P. Jencks, *J. Am. Chem. Soc.* **1991**, *113*, 6997 – 7002; b) E. Grunwald, E. K. Ralph, *Acc. Chem. Res.* **1971**, 107 – 113.
[29] G. Yamamoto, H. Higuchi, M. Yonebayashi, Y. Nabeta, J. Ojima, *Tetrahedron* **1996**, *38*, 12409 – 12420.
[30] a) G. S. Denisov, V. A. Gindin, N. S. Golubev, A. I. Koltsov, S. N. Smirnov, M. Rospenk, A. Koll, L. Sobczyk, *Magn. Reson. Chem.* **1993**, *31*, 1034 – 1037; b) L. Sobczyk, Appl. Magn. Reson. **2000**, *18*, 47 – 61; c) E. R. Johnson, *Magn. Reson. Chem.* **1995**, *33*, 664 – 668.
[31] Gaussian 98 (Revision A.7), M. J. Frisch, G. W. Trucks, H. B. Schlegel, G. E. Scuseria, M. A. Robb, J. R. Cheeseman, V. G. Zakrzewski, J. A. Montgomery, R. E. Stratmann, J. C. Burant, S. Dapprich, J. M. Millam, A. D. Daniels, K. N. Kudin, M. C. Strain, O. Farkas, J. Tomasi, V. Barone, M. Cossi, R. Cammi, B. Mennucci, C. Pomelli, C. Adamo, S. Clifford, J. Ochterski, G. A. Petersson, P. Y. Ayala, Q. Cui, K. Morokuma, D. K. Malick, A. D. Rabuck, K. Raghavachari, J. B. Foresman, J. Cioslowski, J. V. Ortiz, B. B. Stefanov, G. Liu, A. Liashenko, P. Piskorz, I. Komaromi, R. Gomperts, R. L. Martin, D. J. Fox, T. Keith, M. A. Al-Laham, C. Y. Peng, A. Nanayakkara, C. Gonzalez, M. Challacombe, P. M. W. Gill, B. G. Johnson, W. Chen, M. W. Wong, J. L. Andres, M. Head-Gordon, E. S. Replogle, J. A. Pople, Gaussian, Inc., Pittsburgh PA, **1998**.
[32] W. B. Lutz, L. Lasarus, R. J. Meltzer, *J. Org. Chem.* **1962**, *27*, 1695 – 1703.
[33] A. M. Belostotskii, A. B. Shapiro, *Chem. Heterocycl. Compounds* **1984**, 761 – 766.

Received: January 14, 2002 [F3802]

  0947-6539/02/0813-3026 $ 17.50+.50/0